

Project of an autonomous Microgrid with high requirements of reliability for Military Installations

Pedro Jorge Fernandes Domingos

Instituto Superior Técnico, Universidade de Lisboa, Lisbon, Portugal

November 2018

Abstract—Currently, most countries have their critical services based on digital and automatic systems which require an uninterrupted power supply to maintain their functionality. Military forces are also affected by this new paradigm and, as a pillar of national security, they cannot have their operations compromised. Thus, military installations should be modernized in order to reinforce their autonomy and immunity against external factors, such as utility grid outages. In this perspective, microgrid technologies can be applied to enhance the security and operating conditions of military facilities. Within this scope, it is developed a project regarding the Campo Militar de Santa Margarida (CMSM) case study.

As a first step, the CMSM's grid acknowledgement and characterization are carried out, being created a mathematical model to perform a steady-state analysis for different grid operating conditions.

Due to identified technical limitations, some improvements in the existing grid are recommended in order to allow the implementation of a microgrid, being the integration of distributed energy resources (DERs) one of the main issues. According to CMSM's specificity, a biomass power plant becomes the more profitable solution and options for its integration are analyzed.

There is also explored the hypothesis of implementing a microgrid automation system. A set of automatisms, specified and validated using Petri Nets, are proposed to provide an automated management and to intervene over microgrid stability perturbations, being also elaborated some considerations regarding a standardized implementation of automatisms and communication system architecture.

Index Terms—Military Installations, Microgrids, Electrical Grid Modeling and Simulation, Automation, Petri Nets, IEC 61850

I. INTRODUCTION

A. Scope of the work

The actual paradigm reveals that a reliable and fully functional electrical grid is mandatory to ensure the security and economic prosperity in most nations, where public utility grids secure nowadays most of the critical services, such as hospitals, banking, telecommunications and military installations. However, utility grids can be vulnerable to outages due to overloads, atmospheric discharges, faults on transmissions lines or, more recently due to systems digitalization, cyberattacks.

The present work focus on military installations, where are centralized one of the main entities responsible for ensuring the national security within each country - military forces, and, as critical infrastructures, their operations cannot be compromised by external factors. Smart grid technologies, such as microgrids, can assume a key role in reinforcing military facilities security and operating conditions, allowing

their private grids to operate in islanded mode, in other words, disconnected from utility grids. In USA, it is observed a strong interest of Government and National Laboratories in applying microgrid technologies at military installations [1] [2].

When sizing a microgrid with military purposes, it must be taken into account the high security and reliability standards demanded for this type of installations and, simultaneously, implement environmental sustainability policies, such as the integration of renewable DERs and the adoption of energy efficiency measures. The development of a military microgrid project can be divided into the following components:

- **Selection and sizing of DERs**, giving priority to renewable generation sources and integrating diesel generators as conventional emergency backup;
- **Sizing of microgrid's protection and automation system**, provided to ensure the traditional grid protection against faults and to optimize the microgrid operating conditions automatically;
- **Definition of security policies** to guarantee the physical integrity of the facility, but also to ensure the full functionality of its communication and control systems against cyberattacks (cybersecurity measures).

As case study, it is chosen the Campo Militar de Santa Margarida (CMSM), a Portuguese Army's military installation located in the municipality of Constância, Santarém. The CMSM has been in operation since 1952 and has accommodated thousands of soldiers. With 6400 ha of total occupied area, it is one of the largest military installations in Europe and nowadays it stands as the command center of Portuguese Army's Mechanized Infantry Brigade.

B. Motivation and objectives

Due to its central geographical location, CMSM plays a key role in the Portuguese Army's intercommunication between the various military units from north to south of Portugal. However, through the acknowledgement of the CMSM's electrical grid it is noticed that the existing grid is technologically outdated and not in line with the relevance and security requirements of the installation.

The main focus of this work consists in developing a microgrid adapted to the CMSM's needs in order to enhance the security and autonomy of this military installation, with the perspective of this study become extendible to other military facilities in the future.

In the first stage, it is required a previous characterization of CMSM's electrical grid in order to identify its topology, operating conditions, energy consumption patterns and technical limitations. With this technical data, it is elaborated a model to perform a steady-state analysis of the grid for different operating conditions by using *Simulink* tools.

According to CMSM's specificity and to the identified limitations, some changes are proposed to modernize its grid. As first step, it is integrated a biomass power plant as DER, being simulated and analyzed its effects in the grid's behaviour. Then, with the objective of implementing an automation system capable of providing an automated management and ensuring grid stability over perturbations, there are defined the automation principles and requirements for CMSM's microgrid based on its operating conditions.

Within the scope of the microgrid automation system, there are proposed some automatism with the purpose of intervening promptly over different types of grid stability perturbations. The automatism are modelled with Petri Nets, a mathematical tool which provides a set of proprieties used to validate the automatism's functionality and logical flow. Finally, some considerations are made regarding a standardized implementation of automatism and communication and data transmission system architecture, taking into account IEC 61131-3 and IEC 61850 standards, respectively.

II. CMSM'S MEDIUM VOLTAGE GRID

A. Description and Specification

The CMSM owns its private MV distribution grid which supplies the entire military installation. The CMSM's MV grid has an operating voltage of 30 kV and, as can be seen through its single line diagram in Figure 1, it is composed by fifteen MV/LV transformer substations with a total of sixteen transformers and an installed power of 4820 kVA.

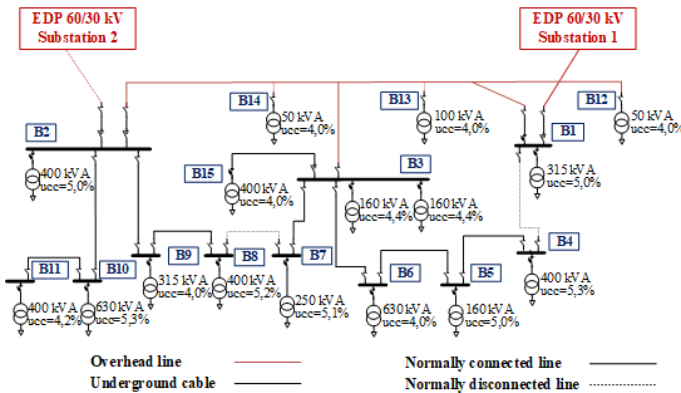


Fig. 1. CMSM's MV grid single line diagram.

1) *MV Grid Topology, Redundancies and Protection philosophy*: This grid is characterized by a mesh grid topology, although always explored as a radial grid and never operated in closed-ring. It can be directly supplied by the public utility grid through two different feeders, existing two interconnection points located respectively in B1 and B2 transformer substations which are never active simultaneously. As the MV grid is operated radially, it has distribution lines which are

normally isolated, guaranteeing redundancies in the supply of the transformer substations within the MV ring. It enables the possibility of exploring the grid with different topologies capable of supplying the entire installation, a fact that allows to prospect a potential automatism to automatically reconfigure the grid's topology after occurring a fault in certain MV lines.

Regarding the actual grid's protection system, it corresponds to a simple and economical but technologically outdated solution. The MV grid's protection is based on switch-fuse combination and load switch-disconnector panels, not existing any switchgear (circuit-breakers) controlled by digital protective relays, in which are based nowadays most of the grids' protection systems. It reveals immediately the technical impossibility of implementing an automated protection system.

2) *MV/LV Transformers*: The MV/LV transformers of the installation have rated powers between 50 - 630 kVA, with impedance voltages of 4% to 6%. In Table I it is shown the ranges of values referred to windings' resistance (R_T), leakage inductance (L_T) and magnetization resistance (R_m) and inductance (L_m), parameters required for transformers' modeling in Simulink, which were calculated applying the typical equations for the transformer's L equivalent circuit.

TABLE I
MV/LV TRANSFORMERS PARAMETERS

Rated Power (kVA)	Rated Voltages (kV)	Z_T (p.u.)	R_T (p.u.)	L_T (p.u.)	R_m (p.u.)	X_m (p.u.)
50		0,040	0,012	0,033	400,0	100,9
to	30 / 0,4	to	to	to	to	to
630		0,053	0,022	0,052	732,6	103,2

3) *MV Distribution Lines*: As can be seen in Figure 1, the interconnections between the different transformer substations are mainly made through underground cables, with average lengths around 500 m. The installed cables are of *LXHIOZI(be)* type, a single core cable type composed by aluminium conductors with a copper wire screen. It also exists an overhead line in CMSM which runs almost its entire length with a total extension of 3,2 km, having terminal points in transformer substations B1 to B3 and B12 to B14. Currently, transmission and distribution overhead lines are typically ACSR (aluminium conductor steel reinforced) conductors, being assumed that the CMSM's overhead line is also from that type. Consulting datasheets and calculation methods from cable manufacturers [3], it can be obtained the essential parameters for modeling the mentioned MV distribution lines in Simulink. In Table II are presented the positive- and zero-sequence resistance (R_1 , R_0), inductance (L_1 , L_0) and capacitance (C_1 , C_0) values for the underground cables and overhead line.

TABLE II
MV DISTRIBUTION LINES PARAMETERS

	R_1 (Ω /km)	R_0 (Ω /km)	L_1 (mH/km)	L_0 (mH/km)	C_1 (F/km)	C_0 (F/km)
Underground cable	0,33	1,27	0,41	1,78	$0,18 \times 10^{-6}$	$0,18 \times 10^{-6}$
Overhead line	0,68	0,82	1,26	4,98	$9,20 \times 10^{-6}$	$4,48 \times 10^{-6}$

4) *Upstream MV Utility Grid*: As previously mentioned, CMSM's MV grid has two interconnection points to the utility

grid. Under normal conditions, the interconnection to the utility grid is made through the B1 transformer substation, being the entrance of B2 used as reserve if the first one fails. Upstream of B1 and B2 are respectively located the HV/MV Substations 1 (Olho de Boi's EDP Substation) and 2 (Almourol's EDP Substation). In order to model the upstream MV utility grid, it is necessary to have information about certain electrical characteristics of HV/MV Substations and the overhead lines which interconnect them to CMSM's grid. For the overhead lines, it is assumed that they are identical to the internal overhead line of CMSM's grid, being its specifications referred in Table II. Consulting a report emitted annually by EDP [4] regarding Distribution Substations, there are obtained the short-circuit powers (S_{cc}) at MV side and neutral earthing system of the mentioned substations, as well as the estimated distances between them and CMSM. In Table III are presented the referred characteristics of HV/MV EDP Substations.

TABLE III
HV/MV EDP SUBSTATIONS TECHNICAL DATA

HV/MV Substation	Rated Voltages (kV)	S_{cc} (MVA)	Neutral system	Distance to CMSM's interconnection point
EDP Substation 1	60 / 30	419	Impedance earthed neutral	22,2 km
EDP Substation 2	60 / 30	172	Impedance earthed neutral	13,1 km

Another necessary input regarding the upstream MV grid is the ratio X/R at the HV/MV Substations location, which corresponds to the relation between the system's reactance and resistance. According to IEC 60909, it can be assumed a value of $X/R = 10$ for grids with operating voltages lower than 35 kV [5].

B. Installation's Energy Consumption

Through the analysis of CMSM's electricity invoices and maximum power consumptions registered on a monthly basis in the installation's energy meter, located at the interconnection point with the utility grid, it can be obtained the electricity consumption fluctuations registered over the year. In Figure 2 are presented the monthly peak load demand at the installation since October 2016 until September 2017.

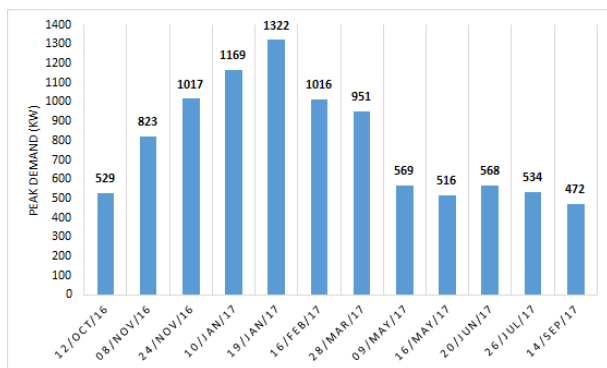


Fig. 2. Monthly peak load demand in CMSM (OCT/2016 - SEP/2017).

During winter months, the average active power demand exceeds 1000 kW, reaching a maximum of 1322 kW in January,

and in summer months the demand decreases around 60%. This variation is mostly explained by a significant increase in the usage of air conditioning systems for heating during winter. Thus, it can be roughly concluded that the installation's peak consumptions in summer are nearly 1/3 of peak consumptions in winter and that 2/3 of winter consumptions are due, in large part, to the usage of heating equipment.

The CMSM's electricity invoices analysis also allowed to conclude that there is no inductive reactive energy billed during the last three years. According to the portuguese reactive energy invoicing legislation for MV consumers [6], inductive reactive energy is only billed if during off-peak periods the average value of $\tan \phi$ is higher than 0,3, corresponding to an average power factor ($\cos \phi$) of 0,958 ind. Consequently, it allows to conclude that CMSM's installation has an average power factor higher than 0,958 ind. measured at the interconnection point with the utility grid.

C. Grid Modeling

In the modeling of the MV grid under analysis, it is used the *SimPowerSystems* [7] toolbox from Simulink, which is composed by a set of libraries and tools that can perform the modeling, simulation and analysis of power systems. In this section are presented the Simulink blocks used to model each component of CMSM's MV grid, as well as the required input parameters.

1) *Transformers*: In Figure 3 it is represented the Simulink block used to model three-phase transformers.

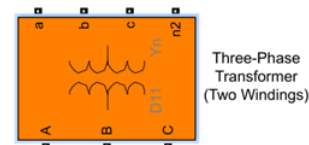


Fig. 3. Transformer Simulink block.

Input parameters:

- Rated power (VA) and grid frequency (Hz);
- Winding parameters - Primary and secondary voltages (V), resistance and leakage inductance (in p.u.);
- Magnetization resistance and inductance (in p.u.).

2) *Distribution lines*: Both distribution line types, underground cables and overhead lines, are modelled using their equivalent Π -model circuit through the Simulink block in Figure 4.

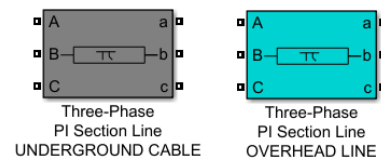


Fig. 4. Three-phase line Simulink block.

Input parameters:

- Grid frequency (Hz);

- Positive- and zero-sequence resistances (Ω/km), inductances (Ω/km) and capacitances (F/km);
- Line length (km).

3) *Upstream grid*: The upstream grid observed from the HV/MV Substations are modelled using the three-phase source Simulink block presented in Figure 5, which replaces an upstream grid by its Thévenin equivalent impedance.

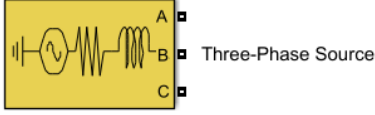


Fig. 5. Three-phase source Simulink block.

Input parameters:

- Rated voltage (V) and grid frequency (Hz);
- Short-circuit power (MVA);
- X/R ratio.

4) *LV consumers*: To model the LV consumers it is used the Simulink block for three-phase RLC loads presented in Figure 6 (highlighted in red). This model allows to agglomerate the consumptions at the LV side of each transformer substation in a single three-phase load, being its active and reactive power consumptions changed according to the simulated installation's power demand.

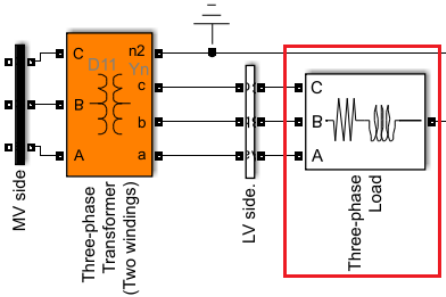


Fig. 6. Three-phase load Simulink block.

Input parameters:

- Rated voltage (V) and grid frequency (Hz);
- Active (W) and reactive (var) power consumptions.

III. BIOMASS POWER PLANT INTEGRATION

In order to improve the resilience of CMSM's installation to utility grid, it is here proposed a biomass power plant as generation source for the microgrid envisioned for CMSM. This choice is primarily justified by the fact of the military installation under study being surrounded by a large forest area, and thus the integration of this renewable generation source would promote the exploration of endogenous resources. When compared with other renewable energy sources, such as wind farms or solar plants, a biomass power plant as a thermoelectric plant has the benefit of being a dispatchable/controlled source which can be used as a combined heat and power (CHP) solution, enabling the possibility of generating electricity and heat simultaneously. Typically, a CHP solution based on a

biomass power plant has a kW_{th}/kW_e ratio equal to 2 - 10 [8].

A biomass CHP power plant is a very interesting solution to enhance the autonomy and energy surety within the CMSM's installation. Simultaneously, it increases the energy efficiency and reduces the installation's electricity demand through the use of the generated thermal energy to provide heating and hot water.

A. Integration Solutions

In this study are analyzed two solutions for the integration of a biomass power plant in the CMSM's grid:

- **Solution A**: The biomass power plant injects its generated power into grid's LV side, using one of the existing transformers with higher rated powers (630 kVA - transformer substations B6 or B10) as interconnection point to MV side. As injection point, it is chosen the existing transformer in B6.

With this solution, it is intended to satisfy the actual CMSM's energy demand. As mentioned previously, the installation's peak load demand is 1332 kW but around 60% of it can be satisfied using thermal energy, which means that only around 40% (~ 570 kW) of total consumption needs to be electrically satisfied. Consequently, the synchronous generator of the biomass power plant should be sized to cover a peak load around 570 kW, being estimated a 700 kVA generator as sufficient to satisfy the installation's electricity demand, as well as the internal consumption and losses of the power plant. Assuming the worst kW_{th}/kW_e ratio, if the biomass power plant injects 570 kW_e into CMSM's grid, it generates at least around 1200 kW_{th} .

- **Solution B**: In this solution, all the power generated by the biomass power plant is injected into grid's MV side, being chosen the MV busbar of the transformer substation B1 as injection point, which is also under normal operating conditions the interconnection point to the utility grid.

This solution is elaborated with the perspective of CMSM's peak load demand suffer a significant growth in the future. Therefore, it is considered a 1600 kVA generator, being assumed that the energy consumption could double if compared with the actual demand. In this case, it is thus necessary a step-up transformer with a rated power in line with the selected generator, in order to interconnect the power plant to B1.

In Figure 7 are illustrated the injection points of the biomass power plant's integration solutions.

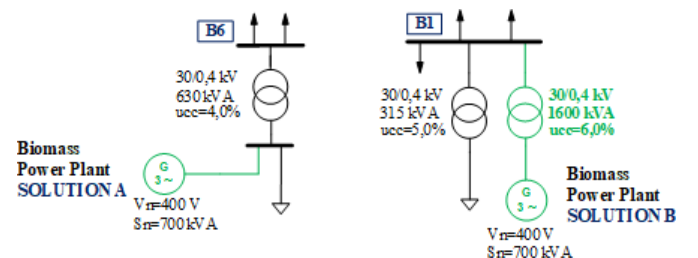


Fig. 7. Biomass power plant's integration solutions.

B. Biomass Power Plant Modeling

In order to model the biomass power plant, there are used a set of Simulink blocks which simulate the dynamic behaviour of each component of the power plant. The biomass power plant Simulink model is represented in Figure 8 and as can be observed, it is defined by a closed-loop system.

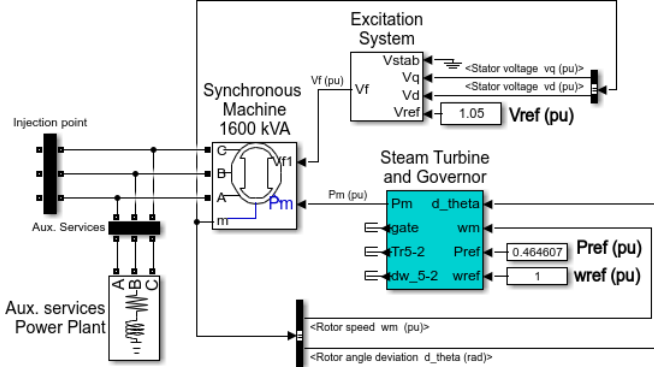


Fig. 8. Biomass power plant Simulink model.

This model is composed by the following components:

- **Synchronous Machine block:** This block models the synchronous generator of the power plant. As main input parameters, the generator model requires its rated power (VA), generation voltage (V) and frequency (Hz). It also requires generator's subtransient, transient and permanent reactances, as well as the respective time constants which define its dynamic behaviour under fault conditions, a set of parameters that can be obtained from manufacturers' datasheets;
- **Excitation system block:** This block implements a DC excitation system that permanently adjusts the generator's output voltage to the desired value (V_{ref}) through the change of its field voltage (V_f). It is applied the default Simulink parametrization used in this block, being only changed V_{ref} to the desired value in simulation.
- **Steam Turbine and Governor block:** This block intends to simulate the operation of biomass power plant's steam turbine and its governor. In this case, it is also applied the default Simulink parametrization, only adjusting the steam turbine's mechanical power (P_{ref}) or speed (w_{ref}) references.

IV. MICROGRID'S LOAD FLOW ANALYSIS

After modelling the different components of the CMSM's microgrid, it is performed the respective load flow (LF) analysis to evaluate the grid's performance for different operating conditions, configurations and load demand scenarios. This analysis has a special focus on how the biomass power plant integration can positively influence the grid's performance.

The LF is computed through the *Load Flow* tool [9] from Simulink, which is used to perform the steady-state analysis of power systems.

A. Load Demand Scenarios

In the microgrid's LF analysis, it is intended to simulate three different load demand scenarios:

- **Demand scenario 1:** This first scenario intends to simulate the actual peak load demand of the installation. As previously mentioned, it corresponds to a maximum power demand of 1322 kW, which is distributed by each transformer substation's LV side, not evenly spread but taking into account the dimension and the current usage of the CMSM's units associated to each transformer substation;
- **Demand scenario 2:** With this scenario it is prospected a more demanding consumption pattern, being considered that each MV/LV transformer of the installation is supplying around 80% of its rated power, corresponding to a power demand around 3500 kVA, more than double of scenario 1. This scenario intends to submit the grid to a peak load demand closer to its total installed power, in order to analyze if the grid's performance still fulfils the installation's power quality standards.
- **Demand scenario 3:** This scenario intends to simulate the actual consumption but considering now that part of them are covered by the heat generated at biomass power plant, which means that the electricity demand drops. Basically, this scenario's consumptions are equal to around 40% of the consumptions reflected on scenario 1, corresponding to a total power demand around 570 kW.

Based on the previous installation's energy consumption analysis, it is assumed $\cos \phi$ equal to 0,93 for LV loads. In Table IV, there are shown the active (P) and reactive (Q) power consumptions registered downstream of the installation's transformer substations for each load demand scenario.

TABLE IV
LOAD DEMAND SCENARIOS

Transformer substation	Scenario 1		Scenario 2		Scenario 3	
	P (kW)	Q (kvar)	P (kW)	Q (kvar)	P (kW)	Q (kvar)
B1	60	24	234	93	26	10
B2	120	47	298	118	52	20
B3	40	15	119	47	17	7
B4	240	95	298	118	103	41
B5	0	0	119	47	0	0
B6	104	41	469	185	45	18
B7	206	81	186	74	89	35
B8	189	75	298	118	81	32
B9	100	40	234	93	43	17
B10	120	47	469	185	52	20
B11	83	33	298	118	36	14
B12	11	4	37	15	5	2
B13	21	8	74	29	9	4
B14	11	4	74	29	5	2
B15	0	0	298	118	0	0

B. Grid's Operating Conditions in LF Simulations

Before proceeding with microgrid's LF simulations, it is necessary to define the grid's operating conditions and load demand scenarios that are being considered in each simulation.

1) **Microgrid's Operating Modes:** It is intended to analyze three different operating modes for the microgrid under study:

- **Current mode:** It corresponds to the operating mode currently applied in CMSM's installation. In this mode, the installation is supplied only by the utility grid and has no DERs integrated;
- **Island mode:** With the biomass power plant's integration, it is now possible to disconnect the installation from the

utility grid and explore it in off-grid modes, maintaining the microgrid fully functional;

- **On-grid mode:** In this mode, the microgrid is supplied in parallel by the biomass power plant and utility grid. Under normal conditions, this is the most advantageous operating mode because it allows to explore the biomass power plant at its rated capacity and any potential surplus of generated energy is injected in the utility grid, ensuring an increased microgrid's energy surety and benefiting in economic terms;

2) *Voltage profiles adjustment:* In order to adjust the grid's voltage profiles, in LF simulations are considering the following operating conditions:

- **Tap changers of MV/LV transformer:** Typically, distribution transformers are equipped with off-load tap changers on primary side with a range of $\Delta U = \pm 5\%$ in steps of 2,5%, which are useful to adjust the voltage profiles relatively close to the LV consumers. In simulations with the load demand scenarios 1 and 3, it is assumed that the transformers are being operated at their nominal taps. In load demand scenario 2, as it corresponds to a significantly more demanding consumption pattern, it is adjusted the tap changers' positions to $\Delta U = -5\%$, in order to increase the voltage in installation's LV side;
- **HV/MV Substations' output voltage:** In LF simulations it is assumed that on MV side of HV/MV Substations the output voltage is regulated to 1,05 p.u.;
- **Biomass power plant's output voltage:** In LF simulations considering the microgrid's island mode, it is assumed that the output voltage of the biomass power plant's synchronous generator is regulated to 1,03 p.u.

C. LF Simulation Results

LF simulation results are presented in Tables V, VI and VII, each one associated to a different load demand scenario. For each LF simulation is visualized the power consumed from the utility grid (P_Q , Q_Q), the power generated by the biomass power plant (P_G , Q_G) and the voltage profiles (V_{MV} , V_{LV}) obtained in installation's MV and LV sides.

TABLE V
LF RESULTS FOR LOAD DEMAND SCENARIO 1

Operating mode	Utility grid's interconnection	Biomass power plant solution	P_Q (kW)	Q_Q (kvar)	P_G (kW)	Q_G (kvar)	V_{MV} (p.u.)	V_{LV} (p.u.)
Current	B1	-	1322	358	-	-	1,02	0,99
	B2	-	1321	353	-	-	1,03	1,01

TABLE VI
LF RESULTS FOR LOAD DEMAND SCENARIO 2

Operating mode	Utility grid's interconnection	Biomass power plant solution	P_Q (kW)	Q_Q (kvar)	P_G (kW)	Q_G (kvar)	V_{MV} (p.u.)	V_{LV} (p.u.)
Current	B1	-	3525	1346	-	-	0,97	0,99
	B2	-	3513	1320	-	-	1,01	1,03
On-grid	B1	A	2879	1275	639	48	0,99	1,01
	B2	A	2869	1254	639	48	1,01	1,04
	B1	B	2113	1305	1428	116	1,00	1,02
	B2	B	2100	1282	1428	116	1,02	1,05

TABLE VII
LF RESULTS FOR LOAD DEMAND SCENARIO 3

Operating mode	Utility grid's interconnection	Biomass power plant solution	P_Q (kW)	Q_Q (kvar)	P_G (kW)	Q_G (kvar)	V_{MV} (p.u.)	V_{LV} (p.u.)
On-grid	B1	A	-61	0	639	48	1,05	1,04
	B2	A	-61	0	639	48	1,05	1,04
	B1	B	-838	-5	1429	116	1,06	1,05
	B2	B	-836	-2	1428	116	1,06	1,05
Island	-	A	-	-	577	48	1,05	1,03
	-	B	-	-	577	58	1,05	1,04

1) *LF results considering load demand scenario 1:* The scenario 1 is applied in LF simulations which consider the grid's current operating mode. The results presented in Table V allow to evaluate the grid's performance for both utility grid's interconnection points, being noticed that for both points the operating voltages obtained in installation's MV and LV sides are similar. It is also important to notice that V_{LV} is around 1 p.u., which is not a robust value because it may occur losses in LV cables between the transformers' LV side and consumers. However, these values can be improved using transformers' tap changers to reduce their turns ratio.

2) *LF results considering load demand scenario 2:* With the scenario 2, there are performed LF simulations for the current and on-grid modes, allowing the possibility of evaluating the biomass power plant's influence in grid's performance. Observing the results in Table VI, it is concluded that microgrid's own generation is contributing to a better voltage profile in CMSM's installation, increasing the values of V_{MV} and V_{LV} in 0,02 - 0,03 p.u.

3) *LF results considering load demand scenario 3:* The scenario 3 is applied to analyze the grid's performance for island and on-grid modes. Through the results shown in Table VII, it can be seen that for the considered load demand scenario the biomass power plant can secure by itself the microgrid's steady-state stability in island mode, providing acceptable values for V_{MV} and V_{LV} , 1,05 p.u. and 1,04 p.u. respectively. In LF simulations considering microgrid's on-grid mode, it is considered that in both integration solutions of the biomass power plant their generators are being explored near their rated capacities, injecting the power surplus in the utility grid, which results in negative values of P_Q . It is also obtained a suitable voltage profile in the installation.

V. SHORT-CIRCUIT CALCULATION IN MICROGRID

With the integration of a biomass power plant in CMSM's grid, it is important to analyze how this new power generation source will contribute to increase the magnitude of short-circuit currents within the microgrid. This analysis intends to evaluate the maximum short-circuit currents for the different microgrid's operating modes, which in most cases are associated to the initial short-circuit currents originated by three-phase symmetrical faults (I''_{k3}) and are useful for sizing the grid's operational equipment in terms of thermal and dynamic stresses' withstand capacities.

A. Short-circuit calculation method

The short-circuit currents are calculated using once more Simulink tools. The block shown in Figure 9 is applied to

simulate a fault occurrence in the different points of the installation, being only necessary to connect it to the desired fault location in microgrid's Simulink model, define the type of short-circuit fault and set the specific simulation time of fault occurrence. Then, it is possible to observe graphically the time evolution of short-circuit currents and voltages.

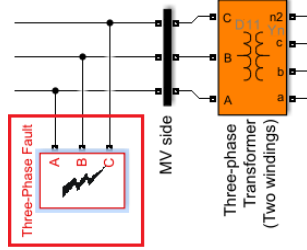


Fig. 9. Three-phase short-circuit fault Simulink block.

B. Short-circuit calculation results

Using the short-circuit calculation method previously detailed, there are calculated the I''_{k3} values simulating faults on MV and LV sides of each transformer substation and considering the different microgrid's operating modes. In Table VIII are presented the range of I''_{k3} values obtained in the microgrid.

TABLE VIII
SHORT-CIRCUIT CURRENTS (I''_{k3}) IN MICROGRID

Operating mode	Utility grid's interconnection	Biomass power plant solution	I''_{k3} (kA)	
			MV	LV
Current	B1	-	0,80 - 0,97	1,81 - 17,81
	B2	-	1,06 - 1,30	1,83 - 18,56
On-grid	B1	A	0,89 - 1,05	1,84 - 25,95
	B2	A	1,11 - 1,38	1,85 - 26,71
	B1	B	0,95 - 1,12	1,85 - 18,49
	B2	B	1,18 - 1,44	1,86 - 19,22
Island	-	A	0,08	1,51 - 4,45
	-	B	0,15	1,63 - 5,57

1) *Results for microgrid's current mode:* Considering the grid's current operating mode, for which the existing grid is dimensioned, the values of I''_{k3} only depend on the utility grid's contribution to fault currents. It is noticed that when comparing the results for both utility grid's interconnection points, the values of I''_{k3} are slightly higher for B2, being obtained short-circuit currents of 0,8 - 1,0 kA when considering B1 and 1,1 - 1,3 kA for B2. This variation is justified because of the difference of lengths between HV/MV Substations and the respective CMSM's interconnection points. Although the short-circuit power in EDP Substation 1 is greater than in EDP Substation 2, the length of the feeder line which interconnects the first substation to B1 is almost twice the length of the second feeder which comes from the second substation, being concluded that for faults on MV side the value of I''_{k3} is essentially limited by feeder lines' impedance. For faults on LV side, it is obtained a range of I''_{k3} between 2 - 18 kA, fault current values which significantly depend of the transformer's impedance.

2) *Results for microgrid's island mode:* Observing the results obtained for the island mode, it can be concluded that the individual contribution of the biomass power plant to fault currents is not significant. On MV side are registered values of I''_{k3} around 80 A and 150 A for biomass power plant's integration solution A and B respectively, being these values limited by the subtransient reactance of power plant's synchronous generator and step-up transformer's impedance. On LV side it is obtained a range of I''_{k3} between 2 - 5 kA.

3) *Results for microgrid's on-grid mode:* As it was observed through the short-circuit analysis for the island mode, the biomass power plant's contribution has a minor influence on short-circuit currents obtained in the microgrid. Therefore, for microgrid's on-grid mode the values of I''_{k3} are quite similar to the ones obtained for the current mode, being the utility grid the major source of fault currents. Consequently, it can be concluded that the existing grid would be able to support the integration of a local power generation source, as the biomass power plant proposed in this work.

VI. MICROGRID'S AUTOMATION PRINCIPLES

With the objective of implementing an automation system to provide a higher autonomy, reliability and security in microgrid's operation and control, a set of automation principles are here proposed for CMSM's microgrid, as well as the required changes in the existing grid which will provide the necessary conditions to integrate a logic of automation functions.

A. Operating principles

In order to define the automation principles which fit the microgrid's needs, it is previously necessary to understand its operating and basic protection requirements.

1) General operating requirements and constraints:

- **Microgrid's operating mode:** Under normal conditions, the microgrid is operated on-grid, being connected in parallel to the utility grid and biomass power plant. Only if occurs a fault or maintenance activities on utility's side or on the power plant, the microgrid's operating mode is changed.
- **Microgrid's topology:** A manual or automatic microgrid's topology reconfiguration cannot create closed rings, being mandatory to preserve its radial structure through the implementation of electrical or mechanical interlocks.
- **Automatic reclosing operations:** Once the existing MV distribution lines in the microgrid are predominantly underground cables, automatic reclosing operations are not practical because an insulation fault in cables are generally permanent and require physical interventions, in contrast to overhead lines.

2) Basic protection requirements:

- **Utility grid - biomass power plant synchronization:** The switch of microgrid's operating modes involves shifting between on-grid and island modes. This operation requires a synchronized reconnection between the microgrid and utility grid, being necessary synchro-check relays to ensure the synchronization conditions automatically through the regulation of biomass

power plant's voltage and frequency to match them with utility grid's. Simultaneously, the biomass power plant should be equipped with a control system which allows to shift its control strategy from P-Q mode when grid-connected, to f-V mode when the microgrid is islanded.

- **Directional overcurrent protection:** As there is the perspective of changing microgrid's topology through automatic reconfigurations, it may cause power flows to reverse their directions. In order to ensure the protection system's coordination and selectivity, there are required directional overcurrent relays in the distribution lines where may occur power flow inversion.
- **Loss-of-mains protection:** In order to prevent the formation of "power islands", which will happen if the utility grid located upstream fails and the microgrid's biomass power plant keeps supplying utility consumers, it is necessary to integrate loss-of-mains relays to recognize this event and immediately disconnect the microgrid from utility grid.

B. Automatism

In order to provide a flexible and dynamic microgrid's control, there are proposed a set of automatisms to intervene over microgrid stability perturbations, mitigate the negative impact faults and restore grid service.

1) *Under Frequency Load Shedding (UFLS):* The UFLS function, typically used in Distribution Substations to act on MV outgoing feeders, reacts to global disturbances in the grid, specifically to the unbalance between generated and consumed power. The Load Shedding aims to restore the grid's balance, with the purpose of avoiding blackouts due to the disconnection of synchronous generators. In CMSM's microgrid, the UFLS can be especially important in island mode, ensuring through load shedding that the installation's load demand do not surpass biomass power plant's generation.

2) *Under Voltage Load Shedding (UVLS):* This function, also typically implemented in Distribution Substations, reacts to the loss of power supply at the busbar level, disconnecting simultaneously all the feeders, which are gradually reconnected only after the normalization of the power supply. The main objective of this function is to avoid a sudden rise of load caused by the simultaneous connection of all loads. The UVLS can also have an important intervention when the CMSM's microgrid is in island mode, preventing the simultaneous connection of all the loads associated to a certain MV busbar of the grid which was previously out of supply, an event that may compromise the biomass power plant stability.

3) *Restoring Operation Automatism (ROA):* The ROA automatism is integrated to provide automatic grid's topology reconfigurations and to intervene when a certain "healthy" busbar of the grid loses its supply due to upstream faults, exploiting new alternative sources of energy to restore the busbar's supply. This function is interesting for CMSM's microgrid because its MV grid has a mesh structure and some supply redundancies, revealing the potential to implement a self-healing automatism, identical to the automatism proposed for MV Grids in [10].

4) *Automatic Microgrid Interconnection (AMGI):* The AMGI automatism is specified in this work specifically for CMSM's microgrid and aims to harness the existence of two utility grid's interconnection points in the microgrid, also designated as points of common coupling (PCC). When occurs the disconnection of the microgrid from the utility grid, the AMGI automatically evaluates new possibilities of reconnecting, starting to evaluate the microgrid stability in island mode. Then, through the analysis of the state of both PCC's, this function takes the decision of reconnecting or not to the utility grid.

The AMGI has the following operating requirements:

- 1) The AMGI only starts its operation after a non-intentional disconnection of the microgrid from utility grid. If the disconnection was ordered by the grid's operator, the function stays on standby and do not intervene.
- 2) Then, this function evaluates the microgrid stability in island mode and only after the grid gets stable, the AMGI proceeds with its operation. If the disconnection of the biomass power plant occurs, the AMGI will immediately try to establish a secure reconnection to the utility grid through one of the PCC's in order to avoid a blackout situation.
- 3) If the microgrid stability in island mode is ensured or occurs the disconnection of the biomass power plant, causing a blackout, the AMGI evaluates the state of both PCC's, as well as the state of the feeder lines and the MV busbars that may be involved in the utility grid's reconnection.
- 4) Finally, the function has to decide regarding the PCC over which will occur the reconnection attempt. The AMGI returns to its "rest" state if the reconnection is accomplished, otherwise the entire process is repeated.

In Figure 10 is shown the flow chart which describes the logical operating of the AMGI automatism.

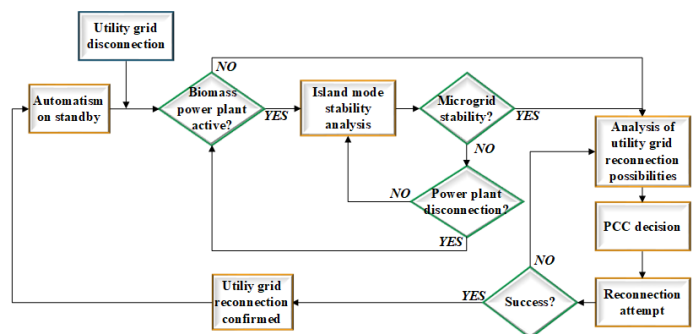


Fig. 10. Flow chart of the AMGI automatism.

C. Modifications in the Existing Grid

Taking into account the existing grid's technical limitations, the implementation of a protection and automation system able to execute the automatisms previously mentioned for CMSM's microgrid, requires in general the following equipment and modifications:

- **Renewal of the primary equipment:** replacement of the existing MV panels by remote-controllable switchgear (circuit breaker panels);
- **Integration of measurement equipment:** it is mandatory to integrate voltage transformers (VT's) and current transformers (CT's) for measuring voltages and currents;
- **Integration of Intelligent Electronic Devices (IED's):** IED's to execute protection relay and automation functions, acquire measurements through VT's and CT's and trip/close circuit breakers;
- **Implementation of a communications and data transmission network:** a communications network for data exchange between the different physical devices which integrate the protection and automation system architecture.

VII. AUTOMATISMS SPECIFICATION WITH PETRI NETS

Petri Nets (PN) are a mathematical tool used to describe the relationship between logical conditions and discrete events, being applied in automatic control systems' modeling and analysis. The PN possesses a set of properties which allow to identify and solve malfunctions and conflicts that may occur in an automation system, being used to validate the correct operating of automation functions. In [11] [12] is justified the application and usefulness of PN in the specification of automatism for Distribution Substations.

Automatism functions such as UFLS, ULVS and ROA were specified and validated in [11] using PN. Following an identical methodology, it is here specified the *Automatic Microgrid Interconnection* (AMGI) automatism with PN.

A. Modeling Automaton

The AMGI automatism requires a continuous verification of the state of the microgrid's elements involved in the interconnection operation: utility grid's feeder lines, microgrid's MV busbars (B1 and B2 transformer substations' busbars) which interconnect directly to the utility grid, and also an overall state of the microgrid's operating mode. Therefore, three modeling automatons are used to specify in PN the operating states of these elements, as well as the events that may cause the change of their states. In Table IX are briefly described the places and states which characterize each modeling automaton.

TABLE IX
MODELING AUTOMATONS' PLACES AND STATES

Microgrid	Feeder line	MV busbar
MR1 On-grid (biomass power plant in operation)	L1 In service	B1 In service
MR2 Islanded and reconnection forbidden	L2 Out of service	B2 Out of service
MR3 Islanded and reconnection allowed	L3 Reconnectable	B3 Reconnectable
MR4 On-grid (biomass power plant disconnected)	L4 Out of service but reconnectable	
MR5 Blackout		

Over the specification in PN of the next AMGI modules, the places and connections associated to the modeling automatons are marked in orange (microgrid automaton), green (feeder line automatons) and blue (MV busbar automatons).

B. Restoring Operation Automatism (ROA)

The ROA automatism was previously specified in PN in [11]. Within the scope of the AMGI automatism, the ROA has the objective of verifying the states of the feeder lines (automatons 1.L and 2.L) and MV busbars (automatons 1.B and 2.B) associated to PCC 1 and PCC 2 respectively, proceeding to an interconnection attempt to the utility grid through an order for closing one of the PCC circuit breakers if the involved elements are in a "healthy" state. In Figure 11 it is shown the specification of the ROA using PN.

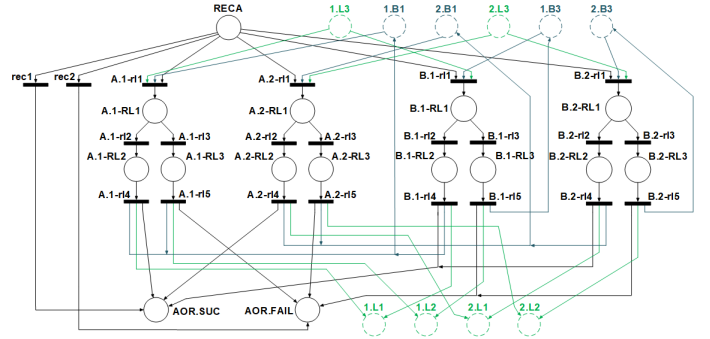


Fig. 11. PN of the ROA, within the scope of the AMGI automatism.

The ROA is composed by two modules (A and B), intervening each one in different operating states of the microgrid, both with the objective of establishing the reconnection to the utility grid. The module A acts when the microgrid shifts to island mode and it is still being supplied by the biomass power plant, while the module B intervenes when occurs a blackout and promptly tries to re-establish the interconnection. The place RECA is the trigger condition of the ROA and, hereafter, it evolves according to microgrid's state and the chosen PCC for the interconnection, being mandatory to set one of the PCC as priority to avoid conflicts. The success or failure of ROA operation is defined by its final states - *AOR.SUC* and *AOR.FAIL*, respectively.

C. Interconnection Management (IM)

Before the actuation of the ROA, the AMGI automatism requires a module to verify continuously the microgrid's overall state and to manage the interconnection attempts to the utility grid when the microgrid shifts non-intentionally to island mode or if occurs a blackout. Therefore, it is specified the IM automatism, which evaluates the microgrid performance and stability and gives permission to ROA to intervene when all the required conditions to reconnect to the utility grid are fulfilled. In Figure 12 it is specified the IM module using PN.

The place *GI.REP* represents the standby state of the IM. When the microgrid disconnects from the utility grid the transition *g1* is transposed, proceeding to a verification of the new microgrid's state in *GI.START*. If it has shifted to island mode (*MR2*), the IM initiates a pause to evaluate the microgrid stability and, if confirmed, it is given the order to ROA operation through marking the place *GI2.A*. On the other hand, if it has occurred a blackout, it is automatically initiated the ROA operation (place *GI2.B* marked). The transitions *gi6*

or $gi7$ are only transposed with the end of ROA operation, meaning respectively the success and failure of the interconnection attempt and returning the IM to standby if successful.

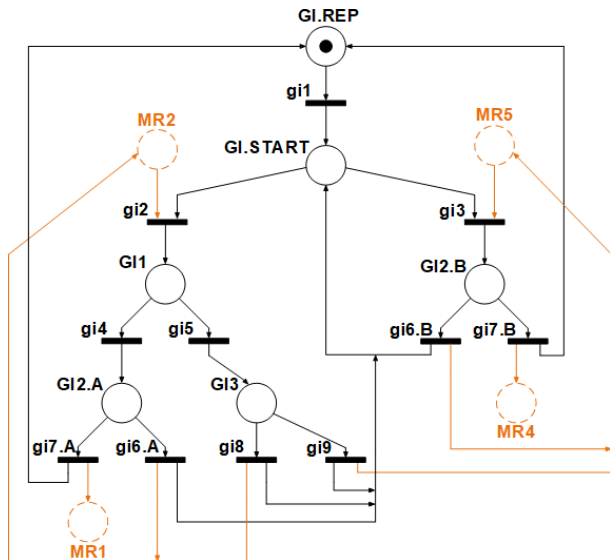


Fig. 12. PN of the IG, within the scope of the AMGI automatism.

D. Considerations regarding the Automatism Implementation

The automatism implementation and the microgrid communication system's architecture should be based on international standards as IEC 61131-3 and IEC 61850, widely applied within power systems, respectively, in the programming of logical controllers (PLC's) and in the definition of the communication protocols which defines the data transmission established between IED's and other physical devices of the system, following an identical methodology to the one proposed in [12].

It is suggested a centralized architecture where a single logical controller, designated as *Microgrid Central Controller* (MGCC) within the scope of microgrids, processes the automatism specified in PN, being the IED's processing capacity applied in the computation of the logical predicates of the automatism. Using existing tools to convert PN in 61131-3 PLC programming languages, it is possible to directly implement the automation functions in the MGCC. In Figure 13, it is illustrated a simplified microgrid system architecture according to IEC 61850.

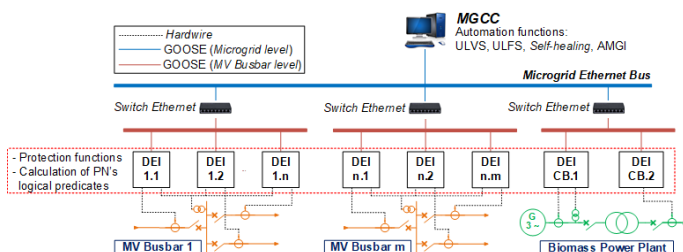


Fig. 13. Microgrid system's architecture: centralized implementation of automatism.

The information from the microgrid's primary equipment is transmitted via hardware to the IED's. The IED's processes the information to compute the necessary logical predicates, which are then transferred to the MGCC through GOOSE messages, an horizontal communication service based on the *publisher-subscriber* principle, provided by IEC 61850. Reversely, the MGCC transmits command orders to IED's to intervene over the primary equipment.

VIII. CONCLUSION

Throughout this paper, an existing MV grid of a military installation (CMSM) is characterized and modelled, being provided a grid's performance analysis through its simulation for different operating conditions. Knowing the grid's specificity and bearing in mind the perspective of implementing a microgrid, it was proposed a biomass power plant as its local generation source to ensure the autonomy and security demanded by the installation and, simultaneously, increase its energy efficiency.

In parallel, there are proposed some modifications based on the existing grid's limitations with the purpose of implementing a protection and automation system, a key component of any modern microgrid's architecture. After the definition of the automation operating principles within the scope of the envisioned microgrid for CMSM, a set of automatism, applied to intervene over microgrid stability perturbations and specified using Petri Nets, are recommended to its automation philosophy with the objective of providing a more reliable, flexible and dynamic management and control of the microgrid and ensuring an uninterrupted power supply to all the parts of the installation, or at least minimize the installation's downtimes.

Finally, some considerations are made regarding a standardized implementation of the automatism and the microgrid's communication system architecture, taking into consideration the conclusions of previous works.

REFERENCES

- [1] *SPIDERS: The Smart Power Infrastructure Demonstration for Energy Reliability and Security*, Sandia National Laboratories, 2012
- [2] Gail Reitenbach, "Military Microgrids: Wanted and Needed but Tough to Deploy", *POWERmagazine*, June 2014.
- [3] *Guia Técnico*, Sodal, Quintas & Quintas, 2007 (in Portuguese).
- [4] *Caracterização das Redes de Distribuição a 31.dez.2017*, Regulamento de Acesso às Redes e às Interligações do Setor Elétrico, EDP Distribuição - Energia, S.A., March 2018 (in Portuguese).
- [5] I. Kasicki, "Short Circuits in Power Systems: A practical Guide to IEC 60909", Wiley-VCH, 2002.
- [6] *Informação sobre faturação de energia reativa: Princípios e boas práticas - Recomendação N. 1/2010*, ERSE, July 2010 (in Portuguese).
- [7] *SimPowerSystems Users Guide*, Version 3, Hydro-Québec, TransÉnergie Technologies, MathWorks, September 2003.
- [8] Rui Castro, "Uma Introdução às Energias Renováveis: Eólica, Fotovoltaica e Mini-hídrica", 2nd Edition, IST Press, 2011 (in Portuguese).
- [9] *SimscapePowerSystems: Load Flow*, Mathworks. Available in: <https://www.mathworks.com/help/physmod/sps/powersys/ref/loadflowbus.html>.
- [10] G. Faria, "Auto-cicatrização de Redes MT sobre CEI 61850", MSc. Thesis, Universidade de Lisboa, April 2014 (in Portuguese).
- [11] J. L. C. Pinto de Sá, "Automatismos Comunicantes em Subestações de Distribuição", PhD Thesis, Universidade Técnica de Lisboa, March 1988 (in Portuguese).
- [12] R. Parreira, "Implementação Normalizada de Automatismos de Subestações de Energia especificados por Redes de Petri", MSc. Thesis, Universidade Técnica de Lisboa, December 2011 (in Portuguese).